COMPRESSIVE 2-D OFF-GRID DOA ESTIMATION FOR PROPELLER CAVITATION LOCALIZATION

Yongsung Park, Peter Gerstoft

Scripps Institution of Oceanography, University of California San Diego, La Jolla, CA, 92093-0238

ABSTRACT

This paper introduces compressive sensing (CS) based two-dimensional (2-D) off-grid direction-of-arrival (DOA) estimation approach which can output the azimuths and elevations of radiating sources for propeller tip vortex cavitation localization. With a discretized angular search-grid of the conventional CS based approach, grid mismatch deteriorates the DOA estimation performance. To obtain the off-grid estimation performance, we formulate the 2-D off-grid DOA estimation problem into a block-sparse CS framework. In addition, the presented method can be applied to arrays of arbitrary geometry with no array configuration constraint. The approach is illustrated by numerical simulations and experimental data (cavitation tunnel experiment).

Index Terms— Compressive sensing, 2-D DOA estimation, 2-D beamforming, Off-grid model

1. INTRODUCTION

To understand ship's radiated noise, localization of the ship noise sources is an important task and noise source localization with a sensor array involves the estimation of two-dimensional (2-D) direction-of-arrivals (DOAs), elevations and azimuths of radiating sources on the array. Propeller cavitation noise is one of the main noise sources of the radiating ship noise [1, 2] and here we focus on the propeller tip vortex cavitation (TVC). We propose a compressive sensing (CS) [3] based framework for estimating 2-D DOAs of the propeller TVC noise sources. The key feature of this localization approach is that as well as offering off-grid DOA estimation, the method is not restricted to a specific array geometry.

Propeller noise localization has been studied in cavitation tunnel experiments [1, 4], including TVC noise source localization [2, 4, 5]. As for localization scheme, matched field processing was utilized. [2, 4] To match the measured acoustic pressure with the replica, which is generated from a potential noise source, replica fields were measured using a virtual source [1] or a ray-based simulation [2]. CS based localization has been applied using that TVC noise is sparse and each source is a monopole. [5]

Supported by the Office of Naval Research, Grant No. N00014-18-1-2118.

To localize the propeller TVC noise, DOAs of the sources on a sensor array can be used. [4] Using the nature of sparsity, CS has been applied for the DOA estimation problem and has shown its good estimation performance. [6, 7, 8] Conventional CS employs a discretized angular grid for DOA estimation and the on-grid CS method degrades from basis mismatch when the true DOAs do not coincide with the angular grid. [9, 10] To overcome the basis mismatch, off-grid CS methods [11] and grid-free CS methods [9, 10] are suggested.

2-D DOA estimation is a classical topics in array processing [12, 13] and CS has been applied. [14, 15, 16] CS based 2-D DOA estimation also suffers from the basis mismatch, and grid-free CS and off-grid CS can be potential solutions. Grid-free CS for multi-dimensional parameter estimation [17, 18] was applied for the 2-D DOA estimation, [19] however, the approach is confined to a uniform rectangular array configuration due to its mathematical framework, and the suggested non-uniform array configuration is not a strictly arbitrary array geometry. Meanwhile, off-grid CS employs a discretized parameter-search grid and approximates the true measurements using first-order Taylor expansion around the grid. [11] The off-grid CS was applied for the 2-D DOA estimation, [20, 21] however, due to its formulational restriction, they divide the 2-D DOA estimation into two 1-D DOA estimations and still assume a specific array configuration.

We base our CS technique upon the off-grid CS approach [11] and solve the 2-D DOA estimation problem without dividing it into the two 1-D problems using the CS of block-sparse signals [22, 23] (we refer to this as block-sparse CS). Using the first-order approximation of the true measurements, the 2-D off-grid DOA estimation problem is expressed into a block-sparse CS framework. The off-grid CS performance is achieved using the block-sparse CS because three components, the discretized angular grid, the difference between the true DOA and the grid concerning the azimuth, and that of elevation, are grouped into a block and are jointly recovered in the block-sparsity enforcing manner.

The key features of the suggested approach are as follows: 2-D off-grid DOA estimation is achieved using block-sparse CS, the approach does not require a specific array configuration and provides the high-resolution capability for propeller TVC localization.

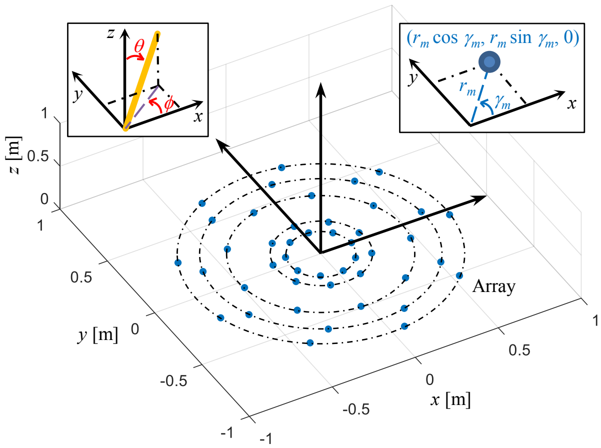

Fig. 1. Array configuration.

2. 2-D OFF-GRID DOA ESTIMATION MODEL

Consider K narrowband far-field sources s_k, $k = 1, \ldots, K$, arriving at an array of M sensors from DOAs (θ_k, ϕ_k), $k = 1, \ldots, K$. The measurement $\mathbf{y} \in \mathbb{C}^M$ is modeled as,

$$\mathbf{y} = \mathbf{A}(\boldsymbol{\theta}, \boldsymbol{\phi})\mathbf{s} + \mathbf{e}, \tag{1}$$

where $\mathbf{y} = [y_1, \ldots, y_M]^\mathsf{T}$, $\boldsymbol{\theta} = [\theta_1, \ldots, \theta_K]^\mathsf{T}$, $\boldsymbol{\phi} = [\phi_1, \ldots, \phi_K]^\mathsf{T}$, $\mathbf{s} = [s_1, \ldots, s_K]^\mathsf{T}$, $\mathbf{e} = [e_1, \ldots, e_M]^\mathsf{T}$, and y_m and e_m, $m = 1, \ldots, M$, are the recorded measurement and measurement noise of the mth sensor respectively. The matrix $\mathbf{A}(\boldsymbol{\theta}, \boldsymbol{\phi}) = [\mathbf{a}(\theta_1, \phi_1), \ldots, \mathbf{a}(\theta_K, \phi_K)]$ is an array manifold matrix and has its columns $\mathbf{a}(\theta_k, \phi_k)$ called steering vector of the kth source whose phase of the entry $a_m(\theta_k, \phi_k)$ contains the delay information of the kth source to the mth sensor.

We are concerned with a 2-D planar array as shown in Fig. 1. Let the $m$the sensor position $(p_{x,m}, p_{y,m}, p_{z,m}) = (r_m \cos\gamma_m, r_m \sin\gamma_m, 0)$, $m = 1, \ldots, M$. The steering vector of the kth source $\mathbf{a}(\theta_k, \phi_k) \in \mathbb{C}^M$ is

$$\mathbf{a}(\theta_k, \phi_k) = \Big[e^{j\frac{2\pi}{\lambda}(p_{x,m}\sin\theta_k\cos\phi_k + p_{y,m}\sin\theta_k\sin\phi_k)}, \ldots, e^{j\frac{2\pi}{\lambda}(p_{x,m}\sin\theta_k\cos\phi_k + p_{y,m}\sin\theta_k\sin\phi_k)}\Big]^\mathsf{T}, \tag{2}$$

where λ is the signal wavelength.

Let $\tilde{\boldsymbol{\theta}} = \{\tilde{\theta}_1, \ldots, \tilde{\theta}_{N_\theta}\}$ be a fixed angular search-grid in the elevation angle range $[-90, 90]^\circ$ and $\tilde{\boldsymbol{\phi}} = \{\tilde{\phi}_1, \ldots, \tilde{\phi}_{N_\phi}\}$ be a fixed angular search-grid in the azimuth angle range $[0, 180]^\circ$, where N_θ and N_ϕ denote the elevation and the azimuth angular search-grid numbers and the elevation and the azimuth angle ranges are divided uniformly with respect to the angular search-grid numbers respectively. Suppose $\theta_k \notin \tilde{\boldsymbol{\theta}} = \{\tilde{\theta}_1, \ldots, \tilde{\theta}_{N_\theta}\}$ and $\phi_k \notin \tilde{\boldsymbol{\phi}} = \{\tilde{\phi}_1, \ldots, \tilde{\phi}_{N_\phi}\}$ for some $k \in \{1, \ldots, K\}$ and that $\tilde{\theta}_{n_k} \in \tilde{\boldsymbol{\theta}}$ and $\tilde{\phi}_{n_k} \in \tilde{\boldsymbol{\phi}}$ are the nearest grid points to θ_k and ϕ_k respectively. Motivated by [11], we approximate the steering vector for the off-grid DOAs $\mathbf{a}(\theta_k, \phi_k)$ using the first-order Taylor expansion,

$$\begin{aligned}\mathbf{a}(\theta_k, \phi_k) &= \mathbf{a}(\tilde{\theta}_{n_k} + \delta\tilde{\theta}_{n_k}, \tilde{\phi}_{n_k} + \delta\tilde{\phi}_{n_k}) \\ &\approx \mathbf{a}(\tilde{\theta}_{n_k}, \tilde{\phi}_{n_k}) + \mathbf{a}_\theta(\tilde{\theta}_{n_k}, \tilde{\phi}_{n_k})\delta\tilde{\theta}_{n_k} + \mathbf{a}_\phi(\tilde{\theta}_{n_k}, \tilde{\phi}_{n_k})\delta\tilde{\phi}_{n_k},\end{aligned} \tag{3}$$

where

$$\mathbf{a}_\theta(\tilde{\theta}_{n_k}, \tilde{\phi}_{n_k}) = \frac{\partial \mathbf{a}(\theta,\phi)}{\partial\theta}\bigg|_{(\tilde{\theta}_{n_k}, \tilde{\phi}_{n_k})},$$

$$\mathbf{a}_\phi(\tilde{\theta}_{n_k}, \tilde{\phi}_{n_k}) = \frac{\partial \mathbf{a}(\theta,\phi)}{\partial\phi}\bigg|_{(\tilde{\theta}_{n_k}, \tilde{\phi}_{n_k})},$$

$\theta_k = \tilde{\theta}_{n_k} + \delta\tilde{\theta}_{n_k}$, and $\phi_k = \tilde{\phi}_{n_k} + \delta\tilde{\phi}_{n_k}$. Denote

$$\mathbf{A}_1 = \Big[\mathbf{a}(\tilde{\theta}_1, \tilde{\phi}_1), \ldots, \mathbf{a}(\tilde{\theta}_1, \tilde{\phi}_{N_\phi}), \mathbf{a}(\tilde{\theta}_2, \tilde{\phi}_1), \ldots, \mathbf{a}(\tilde{\theta}_{N_\theta}, \tilde{\phi}_{N_\phi})\Big] \in \mathbb{C}^{M\times N}$$

$$\mathbf{A}_2 = \Big[\mathbf{a}_\theta(\tilde{\theta}_1, \tilde{\phi}_1), \ldots, \mathbf{a}_\theta(\tilde{\theta}_1, \tilde{\phi}_{N_\phi}), \mathbf{a}_\theta(\tilde{\theta}_2, \tilde{\phi}_1), \ldots, \mathbf{a}_\theta(\tilde{\theta}_{N_\theta}, \tilde{\phi}_{N_\phi})\Big] \in \mathbb{C}^{M\times N}$$

$$\mathbf{A}_3 = \Big[\mathbf{a}_\phi(\tilde{\theta}_1, \tilde{\phi}_1), \ldots, \mathbf{a}_\phi(\tilde{\theta}_1, \tilde{\phi}_{N_\phi}), \mathbf{a}_\phi(\tilde{\theta}_2, \tilde{\phi}_1), \ldots, \mathbf{a}_\phi(\tilde{\theta}_{N_\theta}, \tilde{\phi}_{N_\phi})\Big] \in \mathbb{C}^{M\times N}$$

where

$$\mathbf{a}_\theta(\tilde{\theta}_{n_\theta}, \tilde{\phi}_{n_\phi}) = \frac{\partial \mathbf{a}(\theta,\phi)}{\partial\theta}\bigg|_{(\tilde{\theta}_{n_\theta}, \tilde{\phi}_{n_\phi})}$$

$$\mathbf{a}_\phi(\tilde{\theta}_{n_\theta}, \tilde{\phi}_{n_\phi}) = \frac{\partial \mathbf{a}(\theta,\phi)}{\partial\phi}\bigg|_{(\tilde{\theta}_{n_\theta}, \tilde{\phi}_{n_\phi})}.$$

Note that matrices $\{\mathbf{A}_1, \mathbf{A}_2, \mathbf{A}_3\}$ have $N (= N_\theta \times N_\phi)$ columns. Reordering columns of $\tilde{\mathbf{A}} = [\mathbf{A}_1, \mathbf{A}_2, \mathbf{A}_3] \in \mathbb{C}^{M\times 3N}$ with respect to angles $(\tilde{\theta}_{n_\theta}, \tilde{\phi}_{n_\phi})$, we can represent $\tilde{\mathbf{A}}$ as a concatenation of column-blocks $\tilde{\mathbf{A}}[n]$ of size $M \times 3$,

$$\tilde{\mathbf{A}} = \Big[\underbrace{\mathbf{a}(\tilde{\theta}_1, \tilde{\phi}_1), \mathbf{a}_\theta(\tilde{\theta}_1, \tilde{\phi}_1), \mathbf{a}_\phi(\tilde{\theta}_1, \tilde{\phi}_1)}_{\tilde{\mathbf{A}}[1]}, \underbrace{\mathbf{a}(\tilde{\theta}_1, \tilde{\phi}_2), \mathbf{a}_\theta(\tilde{\theta}_1, \tilde{\phi}_2), \mathbf{a}_\phi(\tilde{\theta}_1, \tilde{\phi}_2)}_{\tilde{\mathbf{A}}[2]}, \ldots, \underbrace{\mathbf{a}(\tilde{\theta}_{N_\theta}, \tilde{\phi}_{N_\phi}), \mathbf{a}_\theta(\tilde{\theta}_{N_\theta}, \tilde{\phi}_{N_\phi}), \mathbf{a}_\phi(\tilde{\theta}_{N_\theta}, \tilde{\phi}_{N_\phi})}_{\tilde{\mathbf{A}}[N]}\Big].$$

Absorbing the approximation error in (3) into the measurement noise, the measurement model in (1) becomes

$$\mathbf{y} = \tilde{\mathbf{A}}\mathbf{x} + \mathbf{e}, \tag{4}$$

where we view $\mathbf{x} \in \mathbb{C}^{3N}$ as a concatenation of N blocks with $\mathbf{x}[n]$ denoting the nth block,

$$\mathbf{x} = [\underbrace{x_1, x_2, x_3}_{\mathbf{x}^\mathsf{T}[1]}, \underbrace{x_4, x_5, x_6}_{\mathbf{x}^\mathsf{T}[2]}, \ldots \underbrace{x_{3N-2}, x_{3N-1}, x_{3N}}_{\mathbf{x}^\mathsf{T}[N]}]^\mathsf{T}$$

for $n = 1, \ldots, N$. By considering $\mathbf{x}$ as a concatenation of blocks, we expect that $\mathbf{x}$ has nonzero entries appearing in blocks, i.e.,

$$\mathbf{x}^{\mathsf{T}}[n] = \begin{cases} [s_k, s_k\delta\tilde{\theta}_{n_k}, s_k\delta\tilde{\phi}_{n_k}], & \text{if } n = n_k \\ & \text{for any } k \in \{1, \ldots, K\} \\ 0, & \text{otherwise.} \end{cases}$$

The recovery of block-sparse vector $\mathbf{x}$ from measurements $\mathbf{y}$ in (4) is the off-grid model to be the focus of this paper. Note that, from $\mathbf{x}[n]$, $\delta\tilde{\theta}_{n_k}$ and $\delta\tilde{\phi}_{n_k}$ are obtained and resultant $\theta_k = \tilde{\theta}_{n_k} + \delta\tilde{\theta}_{n_k}$ and $\phi_k = \tilde{\phi}_{n_k} + \delta\tilde{\phi}_{n_k}$ are followed.

3. 2-D OFF-GRID DOA ESTIMATION WITH BLOCK-SPARSE CS

As discussed in [22], a vector $\mathbf{x} \in \mathbb{C}^{3N}$ is called block k-sparse if $\mathbf{x}[n]$ has nonzero Euclidean norm for at most k indices n. Block-sparsity is defined as $\sum_{n=1}^{N} I\left(\|\mathbf{x}[n]\|_2 > 0\right)$ with the indicator function $I(\cdot)$. A block-sparse solution $\mathbf{x}$ is preferred by minimizing the block-sparsity with the minimization problem

$$\min_{\mathbf{x}} \sum_{n=1}^{N} I\Big(\|\mathbf{x}[n]\|_2 > 0\Big) \quad \text{s.t. } \left\|\mathbf{y} - \tilde{\mathbf{A}}\mathbf{x}\right\|_2 \leq \epsilon, \qquad (5)$$

where ϵ is the noise floor, i.e., $\|\mathbf{e}\|_2 \leq \epsilon$. Unfortunately, dealing with the block-sparsity itself to determine the nonzero blocks in (5) is in general an NP-hard problem. The minimization problem (5) can be relaxed to the closest convex optimization problem and solved efficiently by the minimization problem [22]

$$\min_{\mathbf{x}} \sum_{n=1}^{N} \left\|\mathbf{x}[n]\right\|_2 \quad \text{s.t. } \left\|\mathbf{y} - \tilde{\mathbf{A}}\mathbf{x}\right\|_2 \leq \epsilon. \qquad (6)$$

Herein, we use the CVX program [24] (available in MATLAB) to solve the minimization problem (6). We refer to (6) as block-sparse CS and the l_1-minimization problem [6]

$$\min_{\mathbf{x} \in \mathbb{C}^N} \left\|\mathbf{x}\right\|_1 \quad \text{s.t. } \left\|\mathbf{y} - \mathbf{A}_1\mathbf{x}\right\|_2 \leq \epsilon \qquad (7)$$

as conventional CS.

4. SIMULATION RESULTS

We compare 2-D off-grid DOA estimation results of block-sparse CS with conventional CS. The designed array consists of 5 concentric circles of which the radii range from 0.18 m to 0.75 m. Each circle is composed of 9 hydrophones uniformly separated around the circle. The array configuration is followed by the cavitation tunnel experiment conducted in [4]. We search for sources every $1°$ in elevation $[-90, 90]°$ and azimuth $[0, 180]°$ at frequency $f = 30$ kHz.

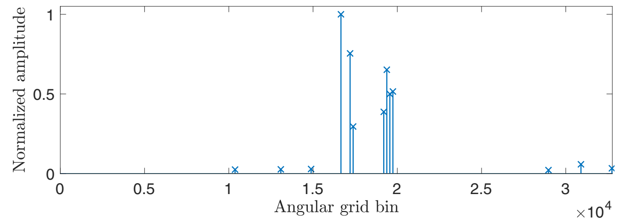

(a) Conventional CS

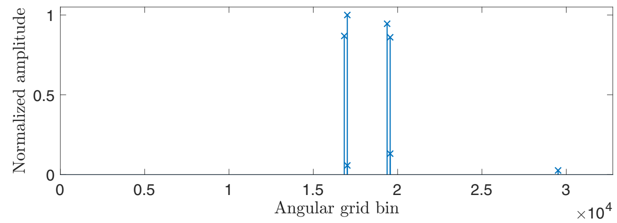

(b) Block-sparse CS

Fig. 2. Activated components of sparse solution $\mathbf{x}$ in 2-D DOA estimation using (a) conventional CS and (b) block-sparse CS. There are two equal strength sources under SNR = 20 dB. Same value of noise floor ($\epsilon = \|\mathbf{e}\|_2$) is used.

$K = 2$ equal strength sources are generated at $(\boldsymbol{\theta}, \boldsymbol{\phi}) = \{(3.5°, 2.5°), (10.5°, 16.5°)\}$. Note that it is the worst case that true DOAs are located right in the middle of grid points. The additive noise is Gaussian noise and the array signal-to-noise ratio (SNR) is used in the simulations, defined as $\text{SNR} = 20\log_{10}(\|\tilde{\mathbf{A}}\mathbf{x}\|_2/\|\mathbf{e}\|_2)$.

Computations were executed on a 2.4 GHz Intel 8-core i9 processor and the averaged time consumptions of block-sparse CS and conventional CS were 126 s and 42 s respectively.

The compelling feature of the presented block-sparse CS is that it utilizes fewer column-blocks than the conventional CS, producing a sparser solution, see Fig. 2. The sparsity is achieved because the block-sparse CS can consider the difference in the steering vectors between the off-grid true DOAs and the corresponding nearest grid points, whereas the conventional CS utilizes more steering vectors to reach the noise floor ϵ.

DOA estimation accuracy tests under 2 grid-intervals ($0.5°$ and $1°$) with 5 SNRs (SNR $= \{0, 5, 10, 15, 20\}$ dB) over 100 trials are considered, see Fig. 3. To consider the case that true DOAs are located right in the middle of grid points, $K = 2$ equal strength sources are generated at $(\boldsymbol{\theta}, \boldsymbol{\phi}) = \{(3.25°, 2.25°), (10.25°, 16.25°)\}$ in the $0.5°$ grid-interval case. Ensemble root-mean-square error (RMSE) is used as a metric to evaluate the estimation accuracy

$$\text{RMSE} = \sqrt{\mathrm{E}\left[\frac{1}{K}\sum_{k=1}^{K}\left(\left(\hat{\theta}_k - \theta_k\right)^2 + \left(\hat{\phi}_k - \phi_k\right)^2\right)\right]}, \qquad (8)$$

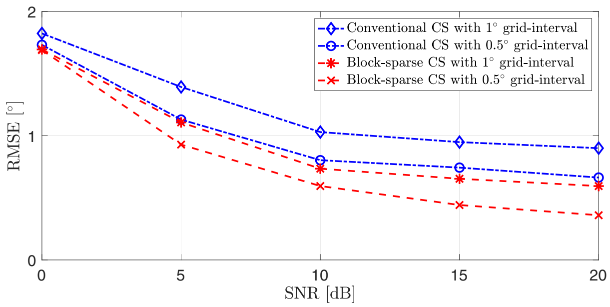

Fig. 3. RMSE [°] comparison between conventional CS and block-sparse CS based 2-D DOA estimation. Each RMSE is averaged over 100 trials.

where $(\hat{\theta}_k, \hat{\phi}_k)$ and (θ_k, ϕ_k) represent the estimated and the true DOAs of the kth source respectively. The presented block-sparse CS is capable of producing higher estimation accuracy than the conventional CS.

5. EXPERIMENTAL RESULTS

In this section, we present the DOA estimation results of the block-sparse CS applied to experimental data from the cavitation tunnel experiment [4] collected on a 45-element planar array, see Fig. 1. The processed data involve the propeller tip vortex cavitation noise and we focused on frequency $f = 35$ kHz among broadband components. For the detailed descriptions and discussions of the experiment and the tip vortex cavitation, see [4].

Conventional beamforming (CBF), $\mathbf{x}_{\text{CBF}} = \mathbf{A}_1^{\mathsf{H}}\mathbf{y}$, conventional CS, and block-sparse CS are compared, see Fig. 4. One noticeable source is detected in many cases. In the vicinity of the peak of CBF in Fig. 4(a), the DOA corresponds to the position of the acoustic center of TVC, which is near the right side of the top center of the propeller when looking upstream. [4, 5]

To show the superior resolution of our approach, we manipulate two datasets having different source locations into one dataset. The CS-based approaches show improved resolution with the sparsity constraint and artifacts in the CBF map are reduced, see Figs. 4(b) and 4(c). Our block-sparse CS approach distinguishes closely located two sources that CBF merges into one peak. The conventional CS estimates one strong source and split another source into two adjacent components that the finer grid can solve.

6. CONCLUSIONS

We provided an introduction to block-sparse CS for 2-D off-grid DOA estimation and its application to propeller TVC noise localization. The proposed scheme is not based on the cutting edge grid-free CS technique, however, we have concentrated on an approach to estimate 2-D parameter jointly in an off-grid manner. The presented method offers quite compelling features: the ability to estimate 2-D DOA in an off-grid manner, no limitation to the array configuration, and the high-resolution capability distinguishing closely located sources.

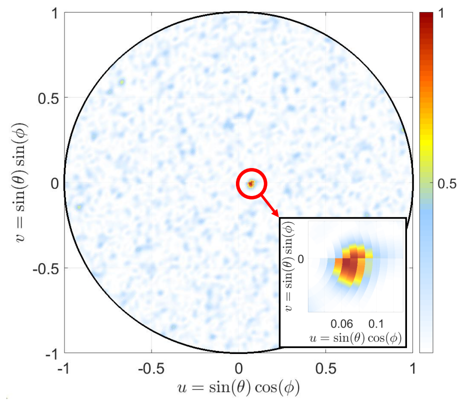

(a) CBF

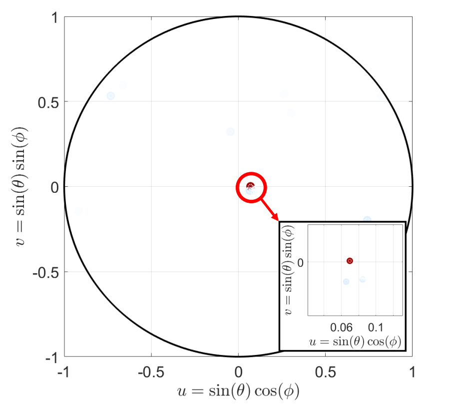

(b) Conventional CS

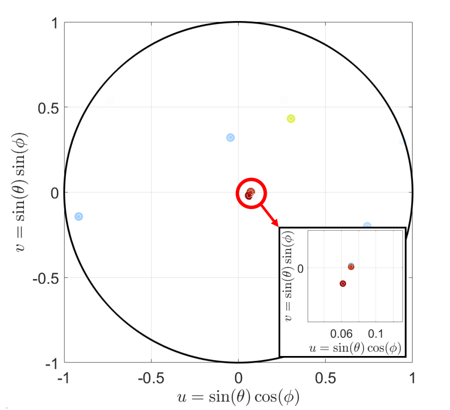

(c) Block-sparse CS

Fig. 4. 2-D DOA estimation for propeller TVC noise localization: (a) CBF, (b) conventional CS, and (c) block-sparse CS.

7. REFERENCES

[1] C. Park, H. Seol, K. Kim, and W. Seong, "A study on propeller noise source localization in a cavitation tunnel," *Ocean Eng.*, vol. 36, no. 9-10, pp. 754–762, 2009.

[2] D. Kim, W. Seong, Y. Choo, and J. Lee, "Localization of incipient tip vortex cavitation using ray based matched field inversion method," *J. Sound Vib.*, vol. 354, pp. 34–46, 2015.

[3] D. L. Donoho, "Compressed sensing," *IEEE Trans. Inf. Theory*, vol. 52, no. 4, pp. 1289–1306, 2006.

[4] C. Park, G. Kim, Y. Park, K. Lee, and W. Seong, "Noise localization method for model tests in a large cavitation tunnel using a hydrophone array," *Remote Sens.*, vol. 8, no. 3, pp. 195, 2016.

[5] Y. Choo and W. Seong, "Compressive spherical beamforming for localization of incipient tip vortex cavitation," *J. Acoust. Soc. Am.*, vol. 140, no. 6, pp. 4085–4090, 2016.

[6] D. Malioutov, M. Cetin, and A. S. Willsky, "A sparse signal reconstruction perspective for source localization with sensor arrays," *IEEE Trans. Signal Process.*, vol. 53, no. 8, pp. 3010–3022, 2005.

[7] A. Xenaki, P. Gerstoft, and K. Mosegaard, "Compressive beamforming," *J. Acoust. Soc. Am.*, vol. 136, no. 1, pp. 260–271, 2014.

[8] P. Gerstoft, A. Xenaki, and C. F. Mecklenbräuker, "Multiple and single snapshot compressive beamforming," *J. Acoust. Soc. Am.*, vol. 138, no. 4, pp. 2003–2014, 2015.

[9] A. Xenaki and P. Gerstoft, "Grid-free compressive beamforming," *J. Acoust. Soc. Am.*, vol. 137, no. 4, pp. 1923–1935, 2015.

[10] Y. Park, Y. Choo, and W. Seong, "Multiple snapshot grid free compressive beamforming," *J. Acoust. Soc. Am.*, vol. 143, no. 6, pp. 3849–3859, 2018.

[11] Z. Yang, L. Xie, and C. Zhang, "Off-grid direction of arrival estimation using sparse bayesian inference," *IEEE Trans. Signal Process.*, vol. 61, no. 1, pp. 38–43, 2012.

[12] C. P. Mathews and M. D. Zoltowski, "Eigenstructure techniques for 2-D angle estimation with uniform circular arrays," *IEEE Trans. Signal Process.*, vol. 42, no. 9, pp. 2395–2407, 1994.

[13] M. D. Zoltowski, M. Haardt, and C. P. Mathews, "Closed-form 2-D angle estimation with rectangular arrays in element space or beamspace via unitary esprit," *IEEE Trans. Signal Process.*, vol. 44, no. 2, pp. 316–328, 1996.

[14] A. M. Elbir and T. E. Tuncer, "2-D DOA and mutual coupling coefficient estimation for arbitrary array structures with single and multiple snapshots," *Digit. Signal Process.*, vol. 54, pp. 75–86, 2016.

[15] J. Shi, G. Hu, X. Zhang, F. Sun, and H. Zhou, "Sparsity-based two-dimensional DOA estimation for coprime array: From sum–difference coarray viewpoint," *IEEE Trans. Signal Process.*, vol. 65, no. 21, pp. 5591–5604, 2017.

[16] S. Nannuru and P. Gerstoft, "2D beamforming on sparse arrays with sparse bayesian learning," in *Proc. IEEE Int. Conf. Acoust., Speech Signal Process. (ICASSP)*. IEEE, May 2019, pp. 4355–4359.

[17] Y. Chi and Y. Chen, "Compressive two-dimensional harmonic retrieval via atomic norm minimization," *IEEE Trans. Signal Process.*, vol. 63, no. 4, pp. 1030–1042, 2014.

[18] Z. Yang, L. Xie, and P. Stoica, "Vandermonde decomposition of multilevel toeplitz matrices with application to multidimensional super-resolution," *IEEE Trans. Inf. Theory*, vol. 62, no. 6, pp. 3685–3701, 2016.

[19] Y. Yang, Z. Chu, Z. Xu, and G. Ping, "Two-dimensional grid-free compressive beamforming," *J. Acoust. Soc. Am.*, vol. 142, no. 2, pp. 618–629, 2017.

[20] J. Li, Y. Li, and X. Zhang, "Two-dimensional off-grid DOA estimation using unfolded parallel coprime array," *IEEE Commun. Lett.*, vol. 22, no. 12, pp. 2495–2498, 2018.

[21] F. F. Shen, Y. M. Liu, G. H. Zhao, X. Y. Chen, and X. P. Li, "Sparsity-based off-grid DOA estimation with uniform rectangular arrays," *IEEE Sens. J.*, vol. 18, no. 8, pp. 3384–3390, 2018.

[22] Y. C. Eldar, P. Kuppinger, and H. Bolcskei, "Block-sparse signals: Uncertainty relations and efficient recovery," *IEEE Trans. Signal Process.*, vol. 58, no. 6, pp. 3042–3054, 2010.

[23] Z. Zhang and B. D. Rao, "Extension of SBL algorithms for the recovery of block sparse signals with intra-block correlation," *IEEE Trans. Signal Process.*, vol. 61, no. 8, pp. 2009–2015, 2013.

[24] M. Grant and S. Boyd, "CVX: Matlab software for disciplined convex programming, version 2.1," 2014, (Last viewed October 1, 2019).